

Electrostatic Spray Ionization Mass Spectrometry Imaging

Liang Qiao,[†] Elena Tobolkina,[†] Andreas Lesch,[†] Alexandra Bondarenko,[†] Xiaoqin Zhong,[†] Baohong Liu,[‡] Horst Pick,[§] Horst Vogel,[§] and Hubert H. Girault^{*,†}

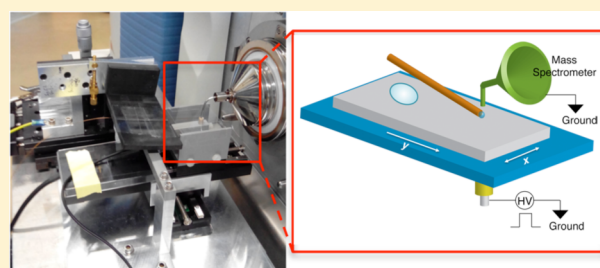
[†]Laboratoire d'Electrochimie Physique et Analytique, Ecole Polytechnique Fédérale de Lausanne, Station 6, CH-1015 Lausanne, Switzerland

[‡]Chemistry Department, Fudan University, 220 Handan Road, 200433 Shanghai, China

[§]Laboratoire de Chimie Physique des Polymères et Membranes (LCPPM), Ecole Polytechnique Fédérale de Lausanne, Station 6, CH-1015 Lausanne, Switzerland

Supporting Information

ABSTRACT: Imaging samples on a surface by mass spectrometry (MS) requires the combination of MS detection with a scanning mode that enables localized desorption and ionization and/or detection of sample analytes with good spatial resolution. We have developed a new mass spectrometry imaging (MSI) method based on electrostatic spray ionization. It works under ambient conditions and can be applied to a wide range of molecules providing quantitative MS analysis even in the presence of salts in excess. 2D MS images of protein and peptide spots, inkjet-printed black dye patterns, and cells were obtained. The presented novel ambient ionization mass spectrometry imaging method can find many applications in analytical and bioanalytical chemistry.



Mass spectrometry imaging (MSI) is a valuable label-free method to investigate the *in situ* distribution of peptides, proteins, metabolites, and drugs in tissues and cells.¹ The most widely used MSI methods include matrix-assisted laser desorption/ionization (MALDI) MSI, laser desorption/ionization (LDI) MSI, secondary ion mass spectrometry (SIMS) imaging, and desorption electrospray ionization (DESI) MSI.¹ MALDI, LDI, and SIMS are normally performed in vacuum, and therefore the corresponding MSI methods are called vacuum MSI methods to distinguish from ambient ionization MSI methods, such as DESI MSI.

The theoretical and instrumental aspects of MSI, together with its applications, have recently been reviewed in several publications.^{1–4} In a typical MSI process, localized mass spectra are recorded sequentially on regular grid points. Plotting the measured relative intensities of individual mass-to-charge ratio (m/z) data with respect to their local positions visualizes the distribution of individual molecules inside a sample such as a tissue slide. The currently most widely used MSI technique is the microprobe mode MSI where the desorption/ionization beam is scanned over the surface or vice versa. Many ionization techniques, such as MALDI, SIMS, LDI and DESI, have been applied in microprobe mode MSI together with mass analyzers, such as time-of-flight (TOF), ion trap, and ion cyclotron, exploiting largely the current developed MS techniques for biological sample imaging.^{3,5,6} However, the microprobe mode imaging process is time-consuming especially when a high spatial resolution is desired.^{3,7} Alternatively, in the microscope mode MSI the ionization is performed from a large area of the surface. Mass analyzers retaining spatial integrity and position sensitive

detectors are employed,^{3,7} rendering the microscope mode MSI theoretically much faster than the microprobe mode MSI. Since the spatial resolution is no longer limited by the desorption/ionization beam, better spatial resolution can be obtained, e.g., a spatial resolution of 4 μm when using a 200 μm laser beam during MALDI MSI.⁷ The microscope mode MSI is now mainly limited by instrumental developments. To date, mainly TRIPLE focusing time-of-flight (TRIFT) has been used as the mass analyzer retaining spatial integrity during microscope mode MSI,⁷ which cannot provide ultrahigh resolution for MS identification of large biological molecules.

Microprobe mode MALDI MSI is the most widely used technique for biological sample MSI because of its good tolerance to salts and the achievable high spatial resolution. The spatial resolution of the microprobe mode MALDI MSI is on the one hand determined by the size of the laser beam, which theoretically cannot be smaller than the wavelength of the light source, and is about 10 μm in practice as achieved for instance with the Bruker ultrafleXtreme MALDI-TOF/TOF. On the other hand, the spatial resolution is determined by the size of the crystals which are generated from the matrix during the sample preparation. For instance, sinapic acid and α -cyano-4-hydroxycinnamic acid are recommended compounds to form small crystals. Alternatively, the dissolution of the matrix in fast evaporating organic solvents results in the deposition of small and uniform matrix crystals on a tissue surface. In another

Received: October 4, 2013

Accepted: January 22, 2014

Published: January 22, 2014

approach, the matrix solution is electrosprayed onto the sample surface to form very small droplets from which the crystals are generated; however, this technique reduces the sensitivity and the reproducibility.⁸ In general, MALDI MSI can reach a spatial resolution of 10 μm ,⁹ but it suffers limitations such as the influence of matrix molecules on the detection in low m/z regions and the limited quantitative analysis, which represent general drawbacks of the MALDI technique.

In contrast to vacuum ionization MSI, a number of ambient ionization methods have been developed for MSI. The major advantage of these ambient ionization MSIs comes from the fact that the surface is sampled with minimal preparation efforts compared to vacuum ionization MSI. At present, the most often used ambient ionization MSI method is DESI MSI, which combines electrospray and desorption ionization.¹⁰ Charged droplets are generated by the electrospray and introduced to a surface containing the sample that is subsequently ionized. DESI involves the initial wetting of the sample surface to dissolve analytes followed by the projection of subsequent droplets with the emission of secondary microdroplets.¹¹ One limitation of DESI MSI is the spatial resolution. Compared to MALDI MSI methods, DESI MSI often operates with a resolution of 180–220 μm ,¹¹ which is caused by the large mist area generated by the electrospray. However, it has recently been demonstrated that the spatial resolution of DESI MSI can be reduced up to 40 μm under particular operating conditions.¹² As reported, the DESI works well only when the analytes are relatively weakly bound to the surface. Its accessible mass range is not comparable to MALDI.¹³ In one application, a tissue section was investigated by DESI for lipid imaging followed by MALDI for protein imaging.¹⁴ Nevertheless, DESI MSI has been applied in the imaging of both artificial sample surfaces and biological tissues.^{15,16}

Another important ambient ionization technique is laser ablation electrospray ionization (LAESI) developed by Nemes, Vertes, and co-workers.¹⁷ LAESI combines the laser desorption of analytes and the ionization of them by the collision of the ablated materials with the charged droplets generated by the electrospray. To date, LAESI has been applied for the MSI of *Aphelandra squarrosa* leaf tissues,¹⁸ rat brain sections,¹⁹ cells in plant tissues,²⁰ and etc. Similar to DESI MSI, the main advantage of LAESI compared to any vacuum MSI is the possibility of working with live samples with only few preparation steps.

Other ambient ionization methods for MSI include liquid extraction surface analysis,²¹ probe electrospray ionization,²² desorption atmospheric pressure photoionization,²³ low-temperature plasma mass spectrometry,²⁴ laser electrospray mass spectrometry,²⁵ and so forth. We have combined scanning electrochemical microscopy (SECM) with MSI by using the so-called push–pull scanner to achieve simultaneous electrochemical reactivity imaging and mass spectrometry imaging, where the latter is a kind of liquid extraction surface analysis MSI.²⁶

Recently, we have introduced the electrostatic spray ionization (ESTASI) as an ambient ionization method to ionize samples on an insulating plate.²⁷ The ESTASI is close to electrospray ionization (ESI) but differs significantly from the ESI in principles and properties: (i) an alternating current high voltage (HV) or pulsed HV is used instead of direct current HV to induce ionization; (ii) instead of directly applying the HV to the sample it is applied to an electrode that is isolated from the sample by an insulator; and (iii) not only solution-based samples but also initially dry samples on a flat surface or inside a porous matrix can

be analyzed under ambient conditions. Therefore, ESTASI is an ionization technique with great flexibility for MS-based chemical and biochemical analysis. Some recent applications include the ionization of samples inside an Eppendorf micropipet tip,²⁷ dried fractions from capillary electrophoresis (CE) on a plastic plate,²⁷ perfume molecules inside a porous smelling paper,²⁸ as well as peptides and proteins in a polyacrylamide gel after isoelectric focusing (IEF).²⁹

Herein, we describe ESTASI for MSI under ambient conditions as a scanning probe technique based on a scanning ESTASI setup and a wetting capillary that delivers constantly nanoliter-droplets of solution for the localized ionization/desorption. This is an innovative ambient ionization mass spectrometry imaging method capable of fully exploiting the specific properties of ionizing dry samples on a surface or inside a porous matrix by the ESTASI. Proof-of-concept results were obtained using ESTASI MSI for surfaces containing representative sample spots and inkjet-printed patterns. The ESTASI MSI works well under a wide molecular mass region for the analysis of organic molecules, peptides, and proteins. It shows tolerance to the presence of salts, provides quantitative analyses with the help of an internal standard, and holds an optimized lateral spatial resolution better than 110 μm . Furthermore, we show that melanoma cells can also be profiled by ESTASI MSI based on the observation of molecules on the surface or inside the cells.

■ EXPERIMENTAL SECTION

Chemicals and Materials. Angiotensin I (Ang I, $\text{NH}_2\text{-DRVYIHPFHL-COOH}$, 98%) was obtained from Bachem (Bubendorf, Switzerland). Nitroated angiotensin I ($\text{NO}_2\text{-AngI}$, $\text{NH}_2\text{-DRVY(nitro)IHPFHL-COOH}$, 98%) was purchased from Eurogentec (Angers, France). Cytochrome c (horse heart, 95%), magnesium chloride hexahydrate (98%), sodium phosphate dibasic dodecahydrate (99%), sodium phosphate monobasic (99%), and sodium chloride (99.5%) were obtained from Fluka (St. Gallen, Switzerland). Methanol (99.9% HPLC grade) was purchased from Applichem GmbH (Darmstadt, Germany). Acetic acid (HAc, 100%) was obtained from Merck (Zug, Switzerland). The Dimatix Model Fluid 003 (Dimatix Fujifilm, Santa Clara, CA) was used as black colorant ink. Polyimide (PI) substrate (125 μm thick, DuPont Kapton HN polyimide film) was obtained from DuPont (Bulle, Switzerland). Calcium chloride (93%) was provided by Sigma-Aldrich (St. Gallen, Switzerland). Potassium chloride (99%) was obtained from Roth AG (Arlesheim, Switzerland). All these reagents and materials were used as received without further purification. Deionized water (18.2 $\text{M}\Omega\text{ cm}$) was obtained from an ultrapure water system (Milli-Q 185 Plus, Millipore) and used for all experiments.

Inkjet Printing. Test samples of a black ink for ESTASI MSI were prepared by inkjet printing of the Dimatix Model Fluid 003 using the DMP-2831 material deposition printer (Dimatix Fujifilm, Santa Clara, CA) and DMC-11610 cartridges with 10 pL nominal drop volume. Printing parameters such as jetting frequency, waveform, drop spacing, and numbers of printed layers were adjusted for optimum printing performance on the PI substrates or a standard photo paper from Epson (Suwa, Japan). After printing on the PI substrates, the ink was dried in a standard oven for 30 min at 200 °C with heating/cooling rate of 1 °C/min.

Cell Culture. The tumorigenic human melanoma cell line WM-115, purchased from ATCC, was cultured in Dulbecco's modified Eagle's medium (Gibco Life Technologies), supplemented with 10% fetal calf serum (FCS) (Gibco Life

Technologies) at 37 °C in humidified atmosphere with 5% CO₂. At 24 h before an experiment, cells were plated at densities of 1 × 10⁵ cells/mL (DMEM/10% FCS) in cell culture dishes (35 mm × 10 mm, Nunc, Denmark).

ESTASI MSI. The ESTASI MSI experiments were performed on an ion trap mass spectrometer (Thermo LTQ Velos, ThermoFisher Scientific, Reinach, Switzerland). The spray voltage of the internal power source of the MS was always set as 0. An enhanced ion trap scanning rate (m/z 10 000 per second) was used. The commercial ESI source was replaced by the ESTASI device. The MS inlet (ion transfer capillary) was modified into an “L” shape where the ion transfer capillary opening was vertically oriented directing downward to facilitate the probing of horizontally mounted samples. In the present work, the analyte samples were deposited by delivering droplets from Eppendorf pipet tips or by inkjet-printing onto thin PI sheets or glossy photo paper that were fixed on an insulating sheet (Gelbond PAG film, 0.2 mm thickness, Amersham Pharmacia Biotech AG, Uppsala, Sweden). The samples were dried under ambient conditions or in an oven before starting the ESTASI MSI analysis. A fused silica capillary (363 μm o.d. and 50 μm i.d. or 150 μm o.d. and 50 μm i.d.) was used to deliver solutions (50% (v/v) methanol, 49% water, and 1% acetic acid) onto the sample under a flow rate of 60 μL/h or 36 μL/h during the ESTASI MSI analysis. The vertical distance between the sample analytes and the MS inlet was 1–3 mm. A custom-made stainless steel microelectrode (radius $r = 100 \mu\text{m}$), upward oriented, was positioned axially with the ion transfer capillary below the sample plate. The microelectrode was always in contact with the insulating sheet to provide a small separation (200–500 μm) from the sample analytes. To induce ESTASI, an amplifying voltage square wave pulse (from 0 V to 9 kV, frequency 5 or 40 Hz, limiting current 0.1 mA) was generated with a high voltage amplifier 10HVA24-P1 (HVP High Voltage Products GmbH, Martinsried/Planegg, Germany) between the microelectrode and the MS inlet. The microelectrode was covered well by the insulating materials preventing from corona or arc discharge events. The integrity of the isolating layer of the microelectrode was intact during all experiments.

MSI of melanoma cells was performed using a similar strategy as for the proteins, peptides, and black ink. Cells were immobilized on a Petri dish. Prior to experiments, the cell culture medium was removed. The Petri dish was washed rapidly three times with phosphate buffered saline (PBS) (10 mM phosphate, 153 mM Na⁺, 4 mM K⁺, 1 mM Ca²⁺, 1 mM Mg²⁺, 144 mM Cl⁻, pH 7.4) and three times with deionized water. After removing all liquid, the adherent cells were dried gently on the bottom of the Petri dish for the ESTASI MSI.

Data analysis was performed by Xcalibur Qual Browser (ThermoFisher Scientific, Reinach, Switzerland). The line scan results were plotted by IGOR Pro (version 6.00 for Macintosh, WaveMetrics, Lake Oswego, OR). 2D-plots of MSIs were generated using the data processing software MIRA (G. Wittstock, University of Oldenburg; <http://www.uni-oldenburg.de/chemie/pc2/pc2forschung/secm-tools/mira/>).

During ESTASI MSI, the microelectrode, the wetting capillary, and the MS inlet were fixed and the substrate was moved laterally with an x,y -positioning system that was constructed by using two perpendicularly oriented MTSS0-Z8 motorized translation stages (Thorlabs, Dachau/Munich, Germany). The movement of the substrate was controlled by an in-house made program developed in Labview (National Instruments, Austin, TX). The substrate was translated with a defined step size and translation

rate. At each step, a delay time was applied for stabilization until the data acquisition of mass spectra had been started.

RESULTS AND DISCUSSION

Ionization Setup for ESTASI MSI. The ESTASI procedure has been described previously in detail.^{27,29} The ionization device

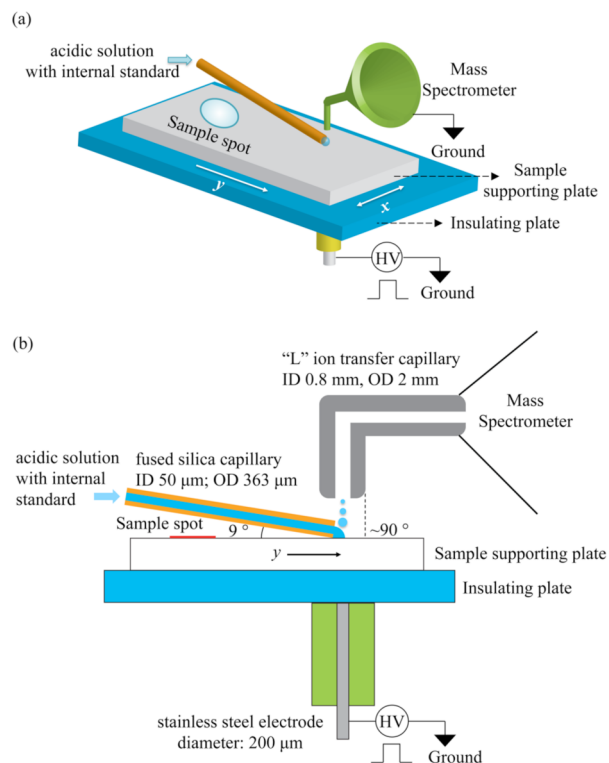


Figure 1. (a) 3D and (b) side view schematic representation of the setup used for ESTASI MSI. HV, high voltage; i.d., inner diameter; o.d., outer diameter. The sample supporting plate is also made of insulating materials and fixed on top of the insulating plate by tapes.

is schematically illustrated in Figure 1. In brief, a sample droplet is deposited onto a substrate under study. One specific area of the sample is positioned underneath the MS inlet and hence above the microelectrode used to provide the pulsed HV. Each time a positive HV is applied to the microelectrode, a spray of cations is evolved from the sample leaving an excess of anions inside the sample droplet after the pulse has been stopped. By grounding the microelectrode, the excess anions are sprayed to neutralize the sample droplet. Continuous voltage square wave pulses (from 0 V to 9 kV) enable the sequential detection of consecutively sprayed cations and anions, respectively.

In order to perform ESTASI MSI, a fused silica capillary was used to wet the substrate locally by depositing a droplet of solution. In this way, the capillary acted as an ink pen to extract samples from the surface (Figure 1). This fused silica capillary was named thereafter the wetting capillary. It was fixed to a holder plate that allowed adjusting accurately an inclination angle γ of the capillary under which it was approached to the substrate and that defined the contact angle between the wetting capillary and the sample surface. This holder was mounted to an x, y, z positioning stage (Thorlabs, Dachau/Munich, Germany) and the capillary was slowly approached toward the sample surface until the mechanical contact was identified using an optical microscope. In all measurements, the capillary was in contact

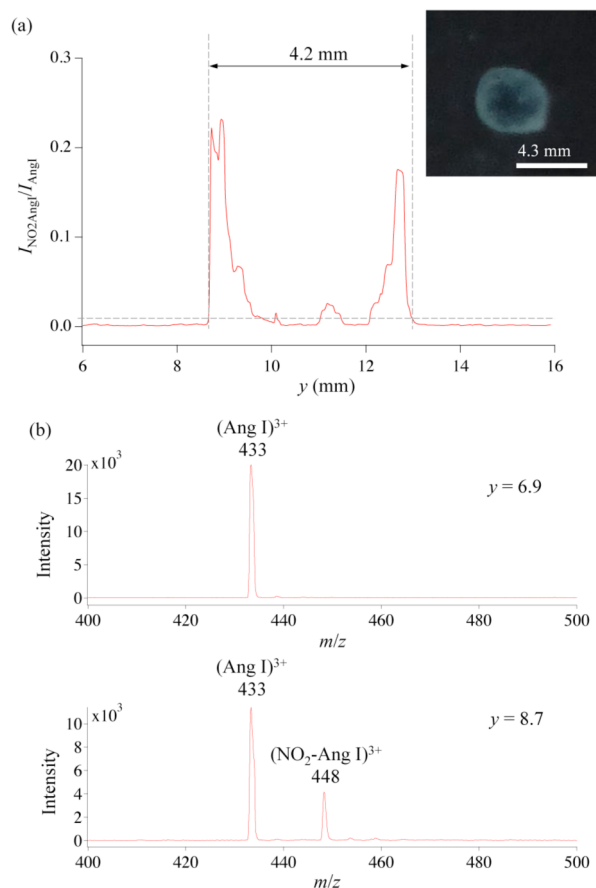


Figure 2. (a) ESTASI MSI y line scan over a NO_2 -Ang I spot. Inset: optical image of the sample spot before the analysis. The signal-to-noise ratio (S/N) in the labeled region >3 . (b) Mass spectra obtained at $y = 6.9$ (mm) and $y = 8.7$ (mm). The NO_2 -Ang I spot was dried from a $5 \mu\text{L}$ droplet of $250 \mu\text{M}$ aqueous NO_2 -Ang I. $(\text{Ang I})^{3+}$, 3 protonated Ang I; $(\text{NO}_2\text{-Ang I})^{3+}$, 3 protonated NO_2 -Ang I. $I_{\text{NO}_2\text{AngI}}$, integrated ion current from m/z 448.0 to m/z 449.0; I_{AngI} , integrated ion current from m/z 433.0 to m/z 434.0. Solution in the wetting capillary 1, Ang I ($150 \mu\text{M}$) in 50% methanol, 49% water, and 1% HAc. Experimental conditions: solution flow rate $60 \mu\text{L/h}$, step size $50 \mu\text{m}$, delay time 1 s, and translation rate 5 mm/s.

with the sample. The capillary opening was placed close to the MS inlet-microelectrode array axis in a way that the delivered droplet position was in-line with the applied electric field. Several relevant parameters, such as the distance between the sample surface and the ion transfer capillary, the inclination angle, the flow rate of the acidic solution inside the wetting capillary, and the frequencies as well as the amplitudes and offsets of the pulsed HV were optimized to obtain good and stable MS signals.

According to a previous study on the ESTASI mechanism,²⁷ a larger distance between the sample droplet and the MS inlet requires a higher voltage to induce the ESTASI. Here, the distance between the sample surface and the MS inlet was 1–3 mm and the HV square wave voltage was 0–9 kV. The frequency of the HV square wave pulse is an important parameter, and the spray of cations is initiated when the applied high voltage is positive, while the spray of anions is generated when the voltage is 0 V (grounded).²⁷ Therefore, the ESTASI is based on a pulsed alternating spray of cations and anions, and the frequency of this pulsed spray is the same as the frequency of the HV square wave. On the other hand, the ion trap mass spectrometry analysis is a pulsed scanning procedure as well. A cycle of analysis includes

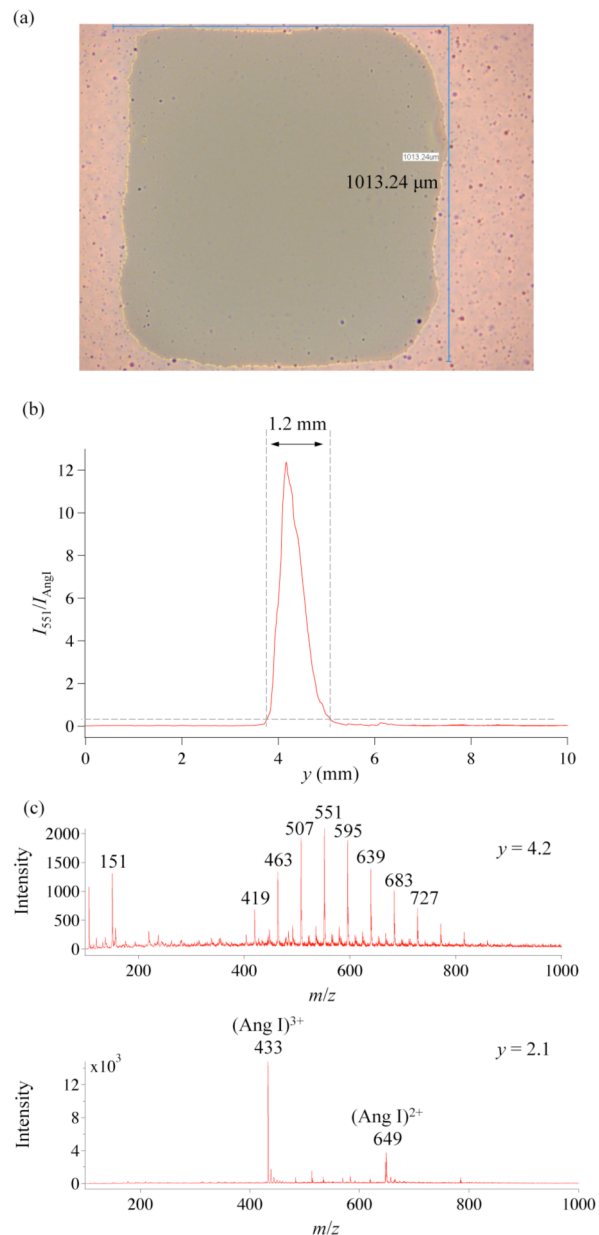


Figure 3. (a) Microscopic image of a printed square of a black ink on a PI substrate ($125 \mu\text{m}$ thickness), the image was made by a laser scanning microscope VK-8710 (Keyence Corporation, Osaka, Japan); (b) ESTASI MSI line scans over the printed black ink using the y line scan mode. (c) Mass spectra obtained at $y = 4.2$ (mm) and $y = 2.1$ (mm). The S/N in the labeled region in part b is bigger than 3. $(\text{Ang I})^{3+}$, 3 protonated Ang I; $(\text{Ang I})^{2+}$, 2 protonated Ang I; I_{551} , integrated ion current from m/z 551.0 to m/z 552.0; I_{AngI} , integrated ion current from m/z 433.0 to m/z 434.0. Solution in the wetting capillary 1, Ang I ($1.5 \mu\text{M}$) in 50% methanol, 49% water, and 1% HAc. Experimental conditions: flow rate of solution $60 \mu\text{L/h}$, step size $50 \mu\text{m}$, delay time 1 s, and translation rate 5 mm/s.

ion injection, ion transfer into the ion trap, scanning of ions by the ion trap, and signal generation on the detector. With the ion trap mass spectrometer, such a cycle takes normally 300–400 ms. In order to get a consecutive MS signal of cations, there must always be at least one spray of cations by ESTASI during the ion injection (max 50 ms) process of each MS analysis cycle, and therefore a high frequency (40 Hz) of the ESTASI or the HV square wave is preferred (see Figure SI-1a in the Supporting

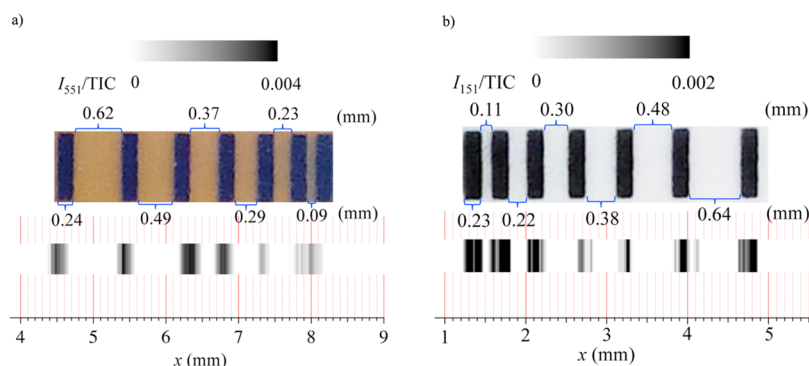


Figure 4. Investigation of the lateral spatial resolution of the ESTASI MSI by using (a) the wetting capillary 1 with 363 μm o.d. and 50 μm i.d. and (b) the wetting capillary 2 with 150 μm o.d. and 50 μm i.d.. The picture shows the inkjet-printed pattern of the black ink on a PI substrate in part a and a glossy photo paper in part b. The ESTASI MSI line scans were plotted to show the distribution of the compounds from the black ink. I_{551} , integrated ion current from m/z 551.0 to m/z 552.0; I_{151} , integrated ion current from m/z 151.0 to m/z 152.0; TIC, total ion current from m/z 300.0 to m/z 800.0. Solution in the wetting capillary, Ang I (1.5 μM) in 50% methanol, 49% water, and 1% HAC. Experimental conditions in part a: solution flow rate 60 $\mu\text{L}/\text{h}$, step size 50 μm , delay time 1 s, and translation rate 5 mm/s. Experimental conditions in part b: solution flow rate 36 $\mu\text{L}/\text{h}$, step size 25 μm , delay time 1 s, and translation rate 5 mm/s.

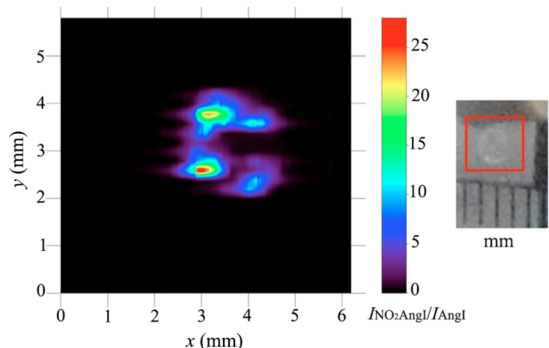


Figure 5. 2D ESTASI MSI of a NO_2 -AngI spot (left) and the optical image of this spot before analysis (right). The NO_2 -AngI spot was dried from a droplet of NO_2 -AngI (1 μL , 25 μM) in methanol. $I_{\text{NO}_2\text{AngI}}$, integrated ion current from m/z 448.0 to m/z 449.0; I_{AngI} , integrated ion current from m/z 433.0 to m/z 434.0. Solution in the wetting capillary 1: Ang I (1.5 μM) in 50% methanol, 49% water and 1% HAC. Experimental conditions: solution flow rate 60 $\mu\text{L}/\text{h}$, step size 200 μm , delay time 1 s, and translation rate 5 mm/s.

Information). In contrast, the intermittent MS signal of cations was obtained when a low frequency (5 Hz) of the HV square wave was employed (Figure SI-1b in the Supporting Information). When the frequency was 5 Hz, there was an interval of 100 ms between each two closest sprays of cations. Because the ESTASI was not synchronized with the ion trap MS analysis, the ion injection (maximum 50 ms) happened sometimes during the spray of cations leading to a strong MS signal of cations, while at other times during the 100 ms interval when anions were generated leading to a very weak MS signal of cations. In all the experiments for MSI, the frequency was set as 40 Hz.

The wetting capillary was brought into a mechanical contact with the substrate by setting the inclination angle to 81° with respect to the surface normal ensuring that the wetting capillary did not block the spray path from the droplet to the MS inlet. During ESTASI MSI, a droplet must always be present at the end of the wetting capillary to contact the sample surface in order to extract analytes for the ionization. At the same time, the droplet should be as small as possible for good spatial resolution and ionization. Therefore, the flow rate of the acidic solution inside

the wetting capillary was adjusted to compensate for solvent evaporation and the ESTASI consumption of the solution. During all MSI experiments, the optimized flow rates were 60 $\mu\text{L}/\text{h}$ for the wetting capillary with 363 μm o.d. and 50 μm i.d. (wetting capillary 1), and 36 $\mu\text{L}/\text{h}$ for the wetting capillary with 150 μm o.d. and 50 μm i.d. (wetting capillary 2), respectively. During all experiments, the relative movements of the capillary in contact with the substrate were accurate and stable due to a certain stiffness of the capillary material.

In order to scan the surface, the substrate was mounted to the x , y translation stages shown in Figure 1a. The y direction was defined as the axis that was in parallel to the wetting capillary while x represented the perpendicular axis. The positions of the MS inlet, the microelectrode and the wetting capillary and hence the solution droplet on the sample surface were kept constant while the sample was translated resulting in a relative capillary movement on the substrate. Sample investigations were performed in three different ways including the x line scan, y line scan and 2D imaging as shown in Figure SI-2 in the Supporting Information. The capillary provides a good stiffness to keep a mechanical contact with the substrate, but it is also flexible enough not to induce scratches into the investigated thin polymer sheets. However, further studies have to be made to determine the influence of the forces that are exerted especially on delicate and weakly anchored analytes. It can be expected that soft samples could be damaged. To overcome this obstacle, x line scans were designed in which the droplet location does not correspond with the capillary contact area (Figure SI-2b in the Supporting Information). Furthermore, this contact area between the sample and the capillary is very small compared to the substrate area that is covered with the liquid droplet. The 2D imaging is a combination of a number of x line scans (Figure SI-2c in the Supporting Information). Therefore, mechanically removed sample analytes are negligible during the ESTASI MSI of the samples investigated herein.

ESTASI MSI Line Scans over Peptide Spots: Quantitative Analysis, Sensitivity, and Tolerance to Salts. To demonstrate the feasibility of using ESTASI for MSI, the y line scan mode (Figure SI-2a in the Supporting Information) was first employed on a spot of NO_2 -Ang I with a diameter of 4.3 mm dried from 5 μL , 250 μM peptide in water. A solution of 150 μM Ang I in 1% acetic acid, 50% water, and 49% methanol was

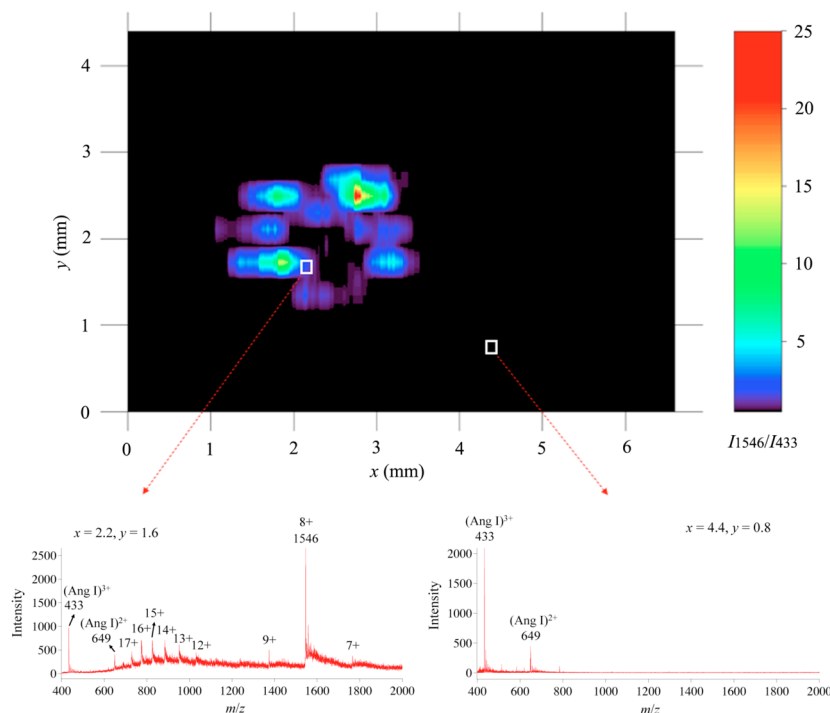


Figure 6. 2D ESTASI MSI of a cytochrome c spot with mass spectra obtained at $x = 4.4$ (mm) $y = 0.8$ (mm) where only Ang I was observed and at $x = 2.2$ (mm) $y = 1.6$ (mm) where both Ang I and cytochrome c were detected. The cytochrome c spot was dried from a droplet of cytochrome c ($1 \mu\text{L}$, $100 \mu\text{M}$) in methanol. I_{1546} , integrated ion current from m/z 1545.5 to m/z 1546.5; I_{433} , integrated ion current from m/z 433.0 to m/z 434.0; $(\text{Ang I})^{3+}$, 3 protonated Ang I; $(\text{Ang I})^{2+}$, 2 protonated Ang I; X^+ , X protonated cytochrome c. Solution in the wetting capillary 1: Ang I ($1.5 \mu\text{M}$) in 50% methanol, 49% water, and 1% HAc. Experimental conditions: solution flow rate $60 \mu\text{L/h}$, step size $200 \mu\text{m}$, delay time 1 s, and translation rate 5 mm/s.

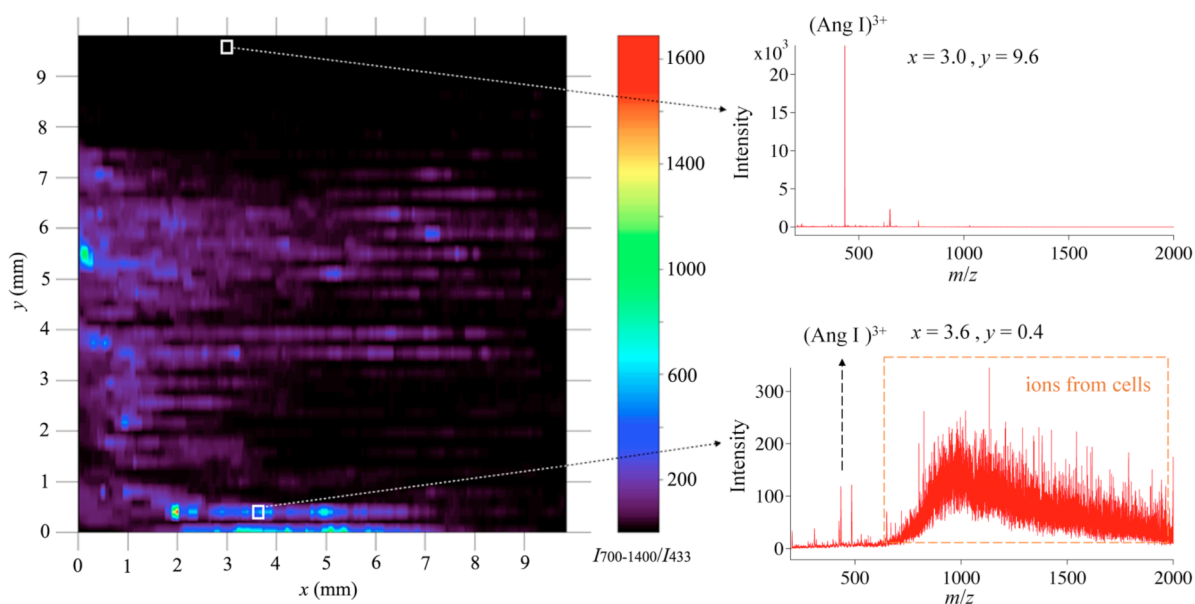


Figure 7. 2D ESTASI MSI of adherent melanoma cells, mass spectrum obtained at $x = 3.0$ (mm) $y = 9.6$ (mm) where only Ang I was observed, and mass spectrum obtained at $x = 3.6$ (mm) $y = 0.4$ (mm) where both Ang I and ions from cells were observed. The melanoma cells were dried on the bottom of the Petri dish before analysis. $I_{700-1400}$, integrated ion current from m/z 700 to m/z 1400; I_{433} , integrated ion current from m/z 433.0 to m/z 434.0; $(\text{Ang I})^{3+}$, 3 protonated Ang I; Solution in the wetting capillary 1, Ang I ($1.5 \mu\text{M}$) in 50% methanol, 49% water, and 1% HAc. Experimental conditions: solution flow rate $60 \mu\text{L/h}$, step size $200 \mu\text{m}$, delay time 1 s, and translation rate 5 mm/s.

delivered by the wetting capillary 1. Ang I was used as an internal standard. Since the amount of NO_2 -Ang I within the sample spot was large, a relatively high concentration of Ang I was used to generate clear peaks in the mass spectra with intensities comparable to NO_2 -Ang I. The quantification of the target

molecules was then performed using the relative intensities (vs the internal standard Ang I) instead of the absolute intensities.

Figure 2a shows the ESTASI MSI line scan over the NO_2 -Ang I spot. Before reaching the NO_2 -Ang I spot, only the 3 protonated Ang I ion was observed on the mass spectra while both the 3 protonated Ang I and the 3 protonated NO_2 -Ang I ions were

observed when ESTASI MS was performed on the NO₂-Ang I spot (Figure 2b). Because of the coffee ring effect, which is a known phenomenon during drying of small droplets (inset in Figure 2a), the concentration of NO₂-Ang I was enriched at the outer rim of the spot (Figure 2a).

The obtained sensitivity in Figure 2 is lower compared to standard ESI or regular ESTASI MS.²⁷ This can be explained for instance by the relatively large droplet size that was used in ESTASI MSI on the substrate for analyte extraction, which results in lower analyte concentrations and more difficult ionization. Moreover, the “L”-shaped, modified ion transfer capillary decreases the sensitivity further. With the modified ion transfer capillary, the MS entrance is vertically oriented directing downward to facilitate the probing of horizontally mounted samples. However, the ion transfer is less efficient because of the 90° turn, resulting in a lower amount of ions entering the ion trap.

In a previous study, we have demonstrated that Ang I and NO₂-Ang I show similar ionization efficiency in ESI, and therefore, their intensity ratio ($I_{\text{NO}_2\text{AngI}}/I_{\text{AngI}}$) obtained by ESI MS is proportional to their concentration ratio.³⁰ The major difference between ESI and ESTASI comes from the way of applying HV to induce the spray, while the ionization processes are quite similar.²⁷ Therefore, ESTASI is also a concentration dependent ionization process. Here, we demonstrated that the relative peak intensities could be used for the quantitative analysis. Four sample spots (2.0 mm in diameter) were prepared by depositing 1 μL of NO₂-Ang I in methanol solution with different concentrations (5 μM, 15 μM, 25 μM, and 30 μM, respectively). The solvent was quickly evaporated, thereby generating spots with a more uniform distribution of NO₂-Ang I on the surface. ESTASI MSI line scans were performed on these spots. A solution of 15 μM Ang I in 1% acetic acid, 50% water, and 49% methanol was delivered by the wetting capillary 1, where the Ang I was used as an internal standard for quantification. Lower concentrations of Ang I were selected since the amounts of NO₂-Ang I in the spots were much smaller than in the spot shown in Figure 2. The relative peak intensities of NO₂-Ang I were calculated as the ratio of the ion current of the 3 protonated NO₂-Ang I (integrated from m/z 448.0 to m/z 449.0) to that of the 3 protonated Ang I (integrated from m/z 433.0 to m/z 434.0). The averaged relative peak intensity of NO₂-Ang I within the 2.0 mm spot region was found to be proportional to the amount of NO₂-Ang I within the sample spot (Figure SI-3 in the Supporting Information), demonstrating that the relative peak intensity can be used for quantitative analysis.

Indeed, when the amount of NO₂-Ang I was reduced up to 2 pmol per spot (2.0 mm diameter, ~0.6 pmol per mm²), the NO₂-Ang I was still detectable by ESTASI MSI but only on a horizontal distance of 0.8 mm with S/N bigger than 3 (Figure SI-4 in the Supporting Information), because the surface concentrations of NO₂-Ang I within the spot were quite low and some parts were too low to be detected by the ESTASI MSI. It should be noticed that the NO₂-Ang I spot was also prepared from a droplet in methanol for a relatively uniform sample surface concentration. The localized ionization took place on an area of approximately 0.03 mm² resulting in ~18 fmol of analyte for ESTASI MS. Introducing wetting capillaries with smaller o.d. and i.d. and optimizing the delivery of the solvents will provide a more efficient analyte extraction and ionization.

Considering a future application of the ESTASI MSI for tissue imaging, the influence of salts on MS signals should be taken into account. In total, 1 nmol of NaCl within a sample spot (2.0 mm in

diameter, containing 25 pmol NO₂-Ang I) did not disturb the MS signal (Figure SI-5a in the Supporting Information) whereas 10 nmol of NaCl in the same sample spot decreased the MS signal significantly (Figure SI-5b in the Supporting Information).

ESTASI MSI Line Scans over Inkjet-Printed Patterns for the Determination of the Spatial Resolution. Inkjet-printed patterns of a black ink were read by the ESTASI MSI and are shown in Figure 3. A square (1 mm × 1 mm, Figure 3a) was generated on a PI substrate (125 μm thickness) and scanned by ESTASI MSI in the y line scan mode (Figure 3b). Before the black ink was reached by the wetting capillary 1, only 3 protonated Ang I ion was observed on the mass spectra since Ang I was delivered by the wetting capillary 1 as an internal label; while a strong peak at $m/z = 151$ and a number of peaks between $m/z = 419$ and $m/z = 727$ representing the black ink were observable when ESTASI MS was performed on the black ink (Figure 3c). The signal from the black ink was obtained over a distance $\Delta y = 1.2$ mm, which is in accordance with the printed square of 1 mm².

The lateral resolution of ESTASI MSI is limited by the size of the droplet that is permanently present at the outlet of the wetting capillary and that is determined by the o.d. and i.d. of the wetting capillary. The wetting capillary 1 with o.d. = 363 μm and i.d. = 50 μm generates droplets with sizes of at least around 200 μm; while the wetting capillary 2 with smaller o.d. (150 μm) and i.d. (50 μm) generates smaller droplets. The experimental studies of the spatial resolution of the ESTASI MSI were performed on a specifically designed and inkjet-printed pattern of the black colorant ink (Figure 4), which included a series of bars with decreasing intervals as indicated on the figure. When scanning such a pattern using an x line scan mode, the lateral spatial resolution was demonstrated to be between 90 and 230 μm for wetting capillary 1 and better than 110 μm for wetting capillary 2, which is consistent with the sizes of the wetting capillaries. Therefore, wetting capillaries with smaller o.d.s should be employed for better spatial resolution. Although Figure 4 shows optimized results achieved with artificially printed patterns, it is expected that real lateral resolution of biological samples will be lower.

Not only the droplet size but also the step size and a so-called tailing effect can influence the spatial resolution and lead to shifted patterns. Such shifts can be found in Figure 4. When a solution droplet has been delivered by the wetting capillary at one specific position without being completely consumed by ESTASI and by solvent evaporation, it will move with the wetting capillary to the next position. Therefore, chemicals from the former position may be analyzed as well, which results in the tailing effect in the regenerated image. Despite flow rate optimization, a complete liquid consumption is hardly detectable with the current setup. On the other hand, an underestimated flow rate could lead to a loss of the MS signal leading to a blank region on the regenerated image. When exchanging the size of the wetting capillaries, the step size and flow rate have to be adjusted in order to achieve a stable performance. In Figure 4b, a smaller step size (25 μm) and a lower flow rate (36 μL/h) were chosen to achieve a higher resolution with wetting capillary 2.

It should be mentioned that much longer data acquisition times are needed for high spatial resolution MSI as for all microprobe mode MSI. In general, a compromise between spatial resolution and experimental time depending on the requirements of the various applications has to be made. The data acquisition time limits MSI especially when using an ion trap

mass spectrometer where the generation of one spectrum with m/z ranges of 100 to 2000 and good resolution takes about 0.3 s.

2D ESTASI MSI. The ESTASI MSI was further applied in a 2D imaging mode of a NO_2 -Ang I peptide spot and alternatively a cytochrome c protein spot. A relatively large step size of 200 μm was selected in accordance with the achievable resolution using wetting capillary 1 (*vide supra* in Figure 5). Ang I was delivered by the wetting capillary as internal standard for quantitative analysis. The obtained ESTASI MSI image of the NO_2 -Ang I spot is shown in Figure 5 and corresponds to the optical image of the dried peptide spot.

In a similar way, the 2D image of a dried cytochrome c spot on a plastic substrate was recorded by ESTASI MSI (Figure 6). The mass spectra showed the strongest peak at 1546 for 8-protonated protein ions correspondingly to a nondenatured structure of cytochrome c.³¹ Thanks to the scanning mode, the cytochrome c spot is immediately dissolved and ionized for MS analysis upon arrival of the wetting capillary keeping low the rate of possible protein denaturation by the used mixture of 50% methanol, 49% water, and 1% HAC.

The analysis of peptide and protein spots has demonstrated that the ESTASI MSI can generate a pattern similar to the optical image with an acceptable spatial resolution. The ESTASI MSI was further applied for imaging adherent melanoma cells from primary tumor (WM 115 cell line). The experiments were performed in a way similar to the ESTASI MSI of protein or peptide spot. Ang I (1.5 μM) in 50% MeOH, 49% H_2O , and 1% acetic acid was delivered as an internal standard by the wetting capillary 1 at a flow rate of 60 $\mu\text{L}/\text{h}$. A step size of 200 μm was chosen during the cell imaging for an area of 1 cm \times 1 cm. Such a step size was chosen to obtain the image in a relatively short time, based on the consideration that the spatial resolution of ESTASI MSI with the wetting capillary 1 was only 90–230 μm under optimized conditions. The initial media for growing cells was completely removed. Then the adherent melanoma cells were washed by PBS buffer and water. Finally, only dried cells on the bottom of the Petri dish were used for ESTASI MSI.

The obtained ESTASI MSI result of melanoma cells on a Petri dish is shown as Figure 7. As a single melanoma cell is very small, it was not possible to observe a single cell with the current setup. However, it was possible to find out if there were many cells or not on the region where ESTASI happened. When there was no cell or only few cells, the obtained spectra showed only the strong signals of Ang I. When there were many cells, signal of ions generated from the cells were observed. At the same time, the peak of Ang I became much weaker as a result of the complex matrix conditions from the cells. With the low-resolution ion trap mass spectrometer, the mass spectra of cells only showed many overlapped peaks in the region m/z 700 to m/z 1400. By plotting the relative integrated intensities of m/z 700 to m/z 1400, the distribution of the adherent cells on the bottom of the Petri dish was obtained. If a high-resolution MS instrument is used, more useful information may be obtained, e.g., to find out biomarkers from different cells.

CONCLUSION AND PERSPECTIVES

A new ambient ionization mass spectrometry imaging technique was developed based on the electrostatic spray ionization. Dried samples, including organic molecules, peptides, proteins, and live cells, could be analyzed with a wetting capillary that is placed in contact with the sample surface and that is translated over the substrate like a scanning probe. It delivers acidic solutions to the sample area under study to extract the analytes for electrostatic

spray ionization. Scanning large areas of a sample gives localized chemical information from a number of mass spectra to generate an image of the distribution of chemicals on the sample surface. Therefore, the ESTASI MSI requires little sample preparation and provides a spatial resolution of the image limited mainly by the inner and outer diameter of the wetting capillary, which could be better than 110 μm under optimized conditions.

Since ESTASI is based on a similar mechanism as ESI with respect to the production of ions from charged droplets, it can be used in the same way for quantitative analysis. ESTASI MSI was developed using an ion trap mass spectrometer with a portable ESTASI source, which makes it easily accessible for many mass spectrometry laboratories. These characteristics of ESTASI MSI demonstrate some advantages over the most widely used MALDI MSI technique.

ESTASI MSI can find many applications in chemical and biochemical analysis and current developments are targeted to the imaging of biological tissues, which includes the optimization of the solution delivered by the wetting capillary for the extraction of specific analytes with high sensitivity and the improvement of the spatial resolution by modifying or replacing the microfluidic devices. ESTASI MSI can find many applications in chemical and biochemical analysis and can be largely improved after further development and optimization.

ASSOCIATED CONTENT

Supporting Information

ESTASI MS signal under low and high frequency HV square wave, move of the sample substrate during ESTASI MSI, quantitative ESTASI MSI, ESTASI MSI of low amount of samples, and ESTASI MSI in the presence of salts. This material is available free of charge via the Internet at <http://pubs.acs.org>.

AUTHOR INFORMATION

Corresponding Author

*E-mail: hubert.girault@epfl.ch.

Author Contributions

The manuscript was written through contributions of all authors. All authors have given approval to the final version of the manuscript.

Notes

The authors declare no competing financial interest.

ACKNOWLEDGMENTS

The authors would like to acknowledge the electronic and mechanic workshops of Institute of Chemical Sciences and Engineering, Ecole Polytechnique Fédérale de Lausanne, for their help in setting up the ESTASI ionization devices. The authors acknowledge Dr. Stockmann for his helpful comments on the manuscript. The Swiss National Science Foundation “Front-end functional microchips for mass spectrometry (Grant 200020-144512)” is acknowledged for funding.

REFERENCES

- (1) van Hove, E. R. A.; Smith, D. F.; Heeren, R. M. A. *J. Chromatogr., A* **2010**, *1217*, 3946–3954.
- (2) Chughtai, K.; Heeren, R. M. A. *Chem. Rev.* **2010**, *110*, 3237–3277.
- (3) McDonnell, L. A.; Heeren, R. M. A. *Mass Spectrom. Rev.* **2007**, *26*, 606–643.
- (4) Wu, C.; Dill, A. L.; Eberlin, L. S.; Cooks, R. G.; Ifa, D. R. *Mass Spectrom. Rev.* **2013**, *32*, 218–243.
- (5) Wiseman, J. M.; Ifa, D. R.; Song, Q. Y.; Cooks, R. G. *Angew. Chem., Int. Ed.* **2006**, *45*, 7188–7192.

- (6) Smith, D. F.; Kiss, A.; Leach, F. E., III; Robinson, E. W.; Pasa-Tolic, L.; Heeren, R. M. A. *Anal. Bioanal. Chem.* **2013**, *405*, 6069–6076.
- (7) Klerk, L. A.; Altelaar, A. F. M.; Froesch, M.; McDonnell, L. A.; Heeren, R. M. A. *Int. J. Mass Spectrom.* **2009**, *285*, 19–25.
- (8) Schwartz, S. A.; Reyzer, M. L.; Caprioli, R. M. *J. Mass Spectrom.* **2003**, *38*, 699–708.
- (9) Jungmann, J. H.; Heeren, R. M. A. *J. Proteomics* **2012**, *75*, 5077–5092.
- (10) Takats, Z.; Wiseman, J. M.; Gologan, B.; Cooks, R. G. *Science* **2004**, *306*, 471–473.
- (11) Ifa, D. R.; Wu, C.; Ouyang, Z.; Cooks, R. G. *Analyst* **2010**, *135*, 669–681.
- (12) Kertesz, V.; Van Berkel, G. J. *Rapid Commun. Mass Spectrom.* **2008**, *22*, 2639–2644.
- (13) Vickerman, J. C. *Analyst* **2011**, *136*, 2199–2217.
- (14) Eberlin, L. S.; Liu, X.; Ferreira, C. R.; Santagata, S.; Agar, N. Y.; Cooks, R. G. *Anal. Chem.* **2011**, *83*, 8366–8371.
- (15) Eberlin, L. S.; Liu, X.; Ferreira, C. R.; Santagata, S.; Agar, N. Y. R.; Cooks, R. G. *Anal. Chem.* **2011**, *83*, 8366–8371.
- (16) Ifa, D. R.; Jackson, A. U.; Paglia, G.; Cooks, R. G. *Anal. Bioanal. Chem.* **2009**, *394*, 1995–2008.
- (17) Nemes, P.; Vertes, A. *Anal. Chem.* **2007**, *79*, 8098–8106.
- (18) Nemes, P.; Barton, A. A.; Li, Y.; Vertes, A. *Anal. Chem.* **2008**, *80*, 4575–4582.
- (19) Nemes, P.; Woods, A. S.; Vertes, A. *Anal. Chem.* **2010**, *82*, 982–988.
- (20) Shrestha, B.; Patt, J. M.; Vertes, A. *Anal. Chem.* **2011**, *83*, 2947–2955.
- (21) Van Berkel, G. J.; Kertesz, V.; Koeplinger, K. A.; Vavrek, M.; Kong, A.-N. T. *J. Mass Spectrom.* **2008**, *43*, 500–508.
- (22) Chen, L. C.; Yoshimura, K.; Yu, Z.; Iwata, R.; Ito, H.; Suzuki, H.; Mori, K.; Ariyada, O.; Takeda, S.; Kubota, T.; Hiraoka, K. *J. Mass Spectrom.* **2009**, *44*, 1469–1477.
- (23) Pol, J.; Vidova, V.; Kruppa, G.; Koblíha, V.; Novak, P.; Lemr, K.; Kotiahov, T.; Kostianen, R.; Havlicek, V.; Volny, M. *Anal. Chem.* **2009**, *81*, 8479–8487.
- (24) Liu, Y.; Ma, X.; Lin, Z.; He, M.; Han, G.; Yang, C.; Xing, Z.; Zhang, S.; Zhang, X. *Angew. Chem., Int. Ed.* **2010**, *49*, 4435–4437.
- (25) Judge, E. J.; Brady, J. J.; Dalton, D.; Levis, R. J. *Anal. Chem.* **2010**, *82*, 3231–3238.
- (26) Momotenko, D.; Qiao, L.; Cortes-Salazar, F.; Lesch, A.; Wittstock, G.; Girault, H. H. *Anal. Chem.* **2012**, *84*, 6630–6637.
- (27) Qiao, L.; Sartor, R.; Gasilova, N.; Lu, Y.; Tobolkina, E.; Liu, B.; Girault, H. H. *Anal. Chem.* **2012**, *84*, 7422–7430.
- (28) Tobolkina, E.; Qiao, L.; Xu, G.; Girault, H. H. *Rapid Commun. Mass Spectrom.* **2013**, *27*, 2310–2316.
- (29) Qiao, L.; Tobolkina, E.; Liu, B.; Girault, H. H. *Anal. Chem.* **2013**, *85*, 4745–4752.
- (30) Qiao, L.; Lu, Y.; Liu, B.; Girault, H. H. *J. Am. Chem. Soc.* **2011**, *133*, 19823–19831.
- (31) Konermann, L.; Douglas, D. J. *Biochemistry* **1997**, *36*, 12296–12302.